

# Behavior of Fused Silica Irradiated by Low Level 193nm Excimer Laser for Tens of Billions of Pulses

C.K. Van Peski<sup>a\*</sup>, Z. Bor<sup>b</sup>, T. Embree<sup>b</sup>, R. Morton<sup>b</sup>

<sup>a</sup> SEMATECH, 2706 Montopolis Dr. Austin, TX 78741

<sup>b</sup> Cymer Inc. San Diego, CA 92127-1815

## ABSTRACT

Fused silica samples from six suppliers were irradiated with a range of fluences ( $0.004\text{mJ}/\text{cm}^2$  to  $0.2\text{mJ}/\text{cm}^2$ ) using an ArF 193nm Excimer laser. The test was performed in an effort to determine fluence level dependency of induced wavefront distortion and birefringence. Each sample was irradiated with four beams of different fluence levels for 22 billion pulses over a period of 133 days. Wavefront distortion in the irradiated areas was observed for all samples. The sign and magnitude of the distortion were dependent upon the fluence level and the particular sample under irradiation. Birefringence measurements were also made. The birefringence characteristic varied among the samples, possibly as a function of fluence level and material. FTIR spectrum measurements were made and were correlated with wavefront distortion measurements. A description of the test and measurements is presented along with data covering a pulse count of 22 billion pulses.

## 1. INTRODUCTION

Fused silica is the material of choice for lenses used in semiconductor lithography equipment operating at 193nm. V. Liberman and others [1,2,3,4] have performed extensive testing of this material at 193nm. Previous work by the Authors [4] reported that low-level, high pulse-count irradiation of less than  $0.1\text{mJ}/\text{cm}^2$  can result in rarefaction, or a decrease of the optical path in the irradiated area. The work reported here seeks to determine the fluence dependency of this rarefaction phenomena. A test was conducted whereby six samples were irradiated by multiple beams covering a range of fluence levels for each sample. Measurements were made of wavefront distortion and birefringence throughout the 22 billion-pulse test. FTIR spectrum measurements were also made of all samples.

## 2. EXPERIMENTAL PROCEDURES

### 2.1 Test facility

A high pulse-rate exposure facility was designed and built by Cymer Inc. using a 2kHz line-narrowed ArF excimer laser. Pulse duration was 15 to 17nsec (integral square pulse duration). The laser was linearly polarized with the E vector of the incident beam horizontal (i.e. parallel with the 40mm side of the samples). A pulse multiplier was constructed of beam splitters, optical delays and beam combiners to produce a 4 kHz pulse train which provided pulse pairs with a 100 nsec temporal separation. An aperture was used to provide a 6mm diameter exposure beam at the input to the samples. An enclosure provided a nitrogen environment for the samples and beam optics.

The test configuration is shown in figure 1. The 4 kHz laser beam enters sample 4 at the lower right and exposes all six samples in series. The beam is then reversed and traversed 20mm by the right-hand turning-prism. Beam two then exposes all six samples in the reverse order, and is then reversed and raised 10mm by the left-hand turning-prism. Beam three exposes all six samples and is finally reversed and shifted by the right-hand turning-prism to become beam 4. In this manner four beams are generated. Bulk absorption and

---

\* Corresponding author. Tel.: +1-512-356-3330 e-mail: [chris.van.peski@sematech.org](mailto:chris.van.peski@sematech.org)

surface losses of the six samples and turning prisms reduce the fluence level of each successive beam by a factor of 2.8. Fluence levels for the samples are given in table 1. Note that sample 4 is exposed to the greatest fluence for beams 1 and 3, whereas sample 22 is exposed to the greatest fluence for beams 2 and 4.

## 2.2 Test samples

Manufacturers of fused silica were asked to provide UV grade fused silica that is designed for the production of high-quality semiconductor lithography lens elements. Sample size was chosen to be 20mm by 40mm by 80mm. The samples were arranged to expose along the 80mm axis. This size and configuration was chosen to provide compatibility with previous tests. Each manufacturer supplied polished samples, so there could be some variation in surface losses, although none was specifically noted. Six samples were selected for the test.

## 2.3 Testing

Exposures were generated at a rate of 4kHz, on a 24-hour, seven-day-week basis with time out for measurement and equipment service. The 22 billion pulses were generated over a period of 133 days. Average daily pulse count was 0.16 billion, and the maximum pulse count in one day was 0.31 billion. Measurements of wavefront distortion and birefringence were made at 2 billion pulse intervals.

## 2.4 Measurement

Birefringence measurements were made using an Exicor™ 150AT. This instrument uses a photoelastic modulator (PEM) to measure magnitude of the birefringence as well as direction of the fast axis. Measurements are made at a wavelength of 632nm.

Wavefront distortion was measured using a Zygo phase-measuring-interferometer (PMI) model GPI-XPHR. This instrument was used in measuring wavefront distortion of the transmitted wave. Flatness measurements of the sample entrance and exit faces were attempted, but no changes were detected within the measurement capability of the instrument, which is in the 3 to 5nm range.

# 3. EXPERIMENTAL RESULTS

## 3.1 Wavefront distortion

Changes in the optical path length of the irradiated areas were noted for all samples to some degree. There was significant variation among samples and, as expected, there was significant variation due to different fluence levels. In general, the change in the optical path length was linear with pulse count.

### 3.1.1 Wavefront distortion beam one

Figure 2 shows the change in path length for laser beam one for all samples. Samples 20, 21 and 22 show an increase in the optical path in the irradiated area. This is normally associated with densification, as has been reported by many researchers [1]. Samples 4,7, and 11 show a decrease in the optical path length. This decrease in optical path, or rarefaction, has been reported previously in fused silica subjected to tens of billions of pulses of low level fluence of less than  $0.1\text{mJ}/\text{cm}^2$  [4]. The change in path length seems reasonably linear with pulse count for all of the samples, but there is a wide variation in slope. This variation is believed to be due primarily to material differences. Samples 4,7 and 11 show a decrease in optical path length, and these samples have the highest fluence for beam one. Samples 21 and 22, with the lowest fluences have the greatest increase in optical path length and have the lowest fluence. This relationship does not hold for beam two however.

### 3.2.2 Wavefront distortion beam two

Distortion resulting from beam two is shown in Figure 3. Note that sample 20, which showed a slight positive change in optical path length for beam one, shows a slight negative change for beam two. This is consistent with previous work where it was shown that fused silica will compact for higher fluences and rarefy for lower fluences [4].

In the region exposed by beam two, samples 21 and 22 have the lower fluence levels, but still show an increase in the optical path. Samples 4, 7, and 11, with the higher fluence levels, still show a decrease in the optical path. It appears that material differences, rather than fluence levels, are the major determinant of behavior. Sample 20 exhibited an increase in the optical path for the higher fluence of beam one, and a decrease in the optical path for the lower fluence level of beam two. The crossover fluence level appears to be dependent upon the material, but we do not understand the material parameters that determine that crossover fluence level.

### 3.2.3 Wavefront distortion beams 3 & 4

The results of beam three are shown in Figure 4. The fluence levels are sufficiently low that five of the samples show rarefaction, and one shows no clear trend. The magnitude of distortion generated by beam three is close the resolution limits of the Zygo interferometer, so the data are noisy. There was some distortion from beam four on some samples, but too small to quantify with confidence.

### 3.3 Birefringence

Birefringence is a condition whereby the optical path length is a function of the polarization of the incident irradiation. Some crystals are naturally birefringent, but in fused silica, birefringence is generally caused by strain in the material. Exposure to 193nm irradiation results in changes in the material density, which cause strain between the exposed and non-exposed regions. This strain ultimately results in birefringence.

Birefringence measurements were made using a Hinds Instrument Exicor 620™. This instrument is capable of mapping the sample and providing both magnitude and direction of the fast axis over a selected grid. Birefringence resolution is 1% for magnitude, and 2 degrees for angle of fast axis. Measurement spot size is 1mm, which provides adequate resolution to measure the 6mm exposed areas. A 1mm grid resolution was selected for all birefringence measurements.

Figure 5 is a 3D representation of birefringence magnitude for sample # 4 after 22 billion pulses. The effects of beam one, two and three are clearly seen. The region exposed by beam one has a birefringence magnitude of 41nm, and is peaked in the center of the exposed area. Beam two region has a maximum birefringence of 3nm and is peaked in an annulus around the exposed area. If a cylindrical volume were uniformly densified, the greatest strain would be an annulus around the periphery of the densified area, as is seen in the region exposed by beam two. The cause of the peak that results from beam one is not clearly understood, but has been reported previously [4].

The birefringence of sample 21 is shown in Figure 6. The birefringence formed by beam one is a sharp peak but has a crater in the center. The reasons for the differences are not understood, but are believed to be related to material differences.

Birefringence as a function of pulse count for all samples is shown in Figure 7. It appears that samples 4 through 20 show a tendency to saturate, with a saturation level that is dependant upon the fluence level. Sample 21 does not show signs of saturation and sample 22 shows a weak tendency toward saturation. We note that there is little correlation between wavefront distortion and birefringence. This is consistent with previously reported results [4].

A second set of birefringence measurements was made after a lapse of 64 days to check for potential relaxation. No significant changes were noted.

### 3.4 FTIR Spectral analysis

An FTIR spectral analysis was performed on the samples at the conclusion of the exposure tests. Measurements were made using a Spectrometer Magna-IR Model 150 manufactured by Nicolet. The samples were measured along the 20mm axis to minimize the IR absorption. Figure 8 shows the spectral response for all samples.

There is a broad absorption peak at  $3650\text{ cm}^{-1}$ . This broad peak is indicative of an OH bond [5]. At this wavelength, absorption through 2cm of material was greater than 99%, so it was not possible to discern differences in absolute absorption among the different samples. There was a difference in the width of the absorption band among the samples however. This feature was used to correlate the FTIR spectrum data with the wavefront distortion. The relationship between absorption-band-width and optical-path length change is shown in Figure 9. Samples with the greater width of the absorption band at  $3650\text{ cm}^{-1}$  have a smaller change in optical path length. Those samples with a greater change in the optical path have a narrower absorption band width. For this correlation, the width of the absorption band was taken at the 10% transmission point. The width of the absorption band may be related to the concentration of OH bonds, but this has not been established.

#### 4. CONCLUSIONS

It appears that there are two separate mechanisms at work. One is a densification process described by Piao [6] as obeying a power law:

$$\frac{\Delta\rho}{\rho} = AD^c$$

Where  $\rho$  is density, D is absorbed dose and A and c are constants. Piao [6] notes that constant c is about 2/3 for UV irradiation. This relationship does not seem to describe irradiation by low fluence levels where the change in density,  $\frac{\Delta\rho}{\rho}$  appears to be negative. There may be a second mechanism at work which is a

one-photon process that results in a rarefaction. The proposed one-photon process would dominate for low fluence levels, resulting in a rarefaction and a decrease in the optical path length. At high fluences, the two-photon process would dominate and would result in densification and an increase in the optical path length.

It is difficult to quantify this proposed second mechanism, because it requires very low fluence levels to minimize the effects of the two-photon process, which requires many tens of billions of pulses.

There is also a strong material dependency as is seen in the widely disparate results from the different samples of this test.

#### ACKNOWLEDGEMENTS

We thank the material suppliers for providing the test samples and for their valuable insights and suggestions. They shall remain nameless at this time by their choice. Our thanks also to M. Rothschild, and V. Liberman, of Massachusetts Institute of Technology, Lincoln Laboratory, for their discussions and ideas. We also thank W. Carlos of Naval Research Laboratory for conducting the FTIR measurements and assisting in the interpretation.

#### REFERENCES

1. V. Liberman, M. Rothschild, J.H.C. Sedlacek, R.S. Uttaro, A. Grenville, "Excimer-laser-induced densification of fused silica: laser-fluence and material-grade effects on the scaling law," *J. Non-Cryst. Solids* **244**, 159-171, 1999.

2. T.T. Seward, D. Smith, N.F. Borrelli, D.C. Allan, "Densification of synthetic fused silica under ultraviolet irradiation," *J. Non-Cryst. Solids* **222**, pp. 407-414, 1997.
3. V. Liberman, M. Rothschild, J.H.C. Sedlacek, R.S. Uttaro, A. Grenville, A.K. Bates, C.K Van Peski, "Testing of optical materials for 193nm applications," *Proc. SPIE* **3427** 411-418, 1998.
4. C.K. Van Peski, R. Morton, Z. Bor, "Behavior of fused silica irradiated by low level 193 nm excimer laser for tens of millions of pulses," *J. Non-Cryst. Solids* **265**, pp. 285-289, 2000.
5. B. Stuart, *Modern Infrared Spectroscopy*, pp. 55-56, John Wiley & Sons, New York, 1996
6. F. Piao, William Oldham, E Haller, "The mechanism of radiation-induced compaction in vitreous silica," *J. Non-Cryst. Solids* **000**, pp. 1-11, 2000.

Fluence levels (mJ/cm<sup>2</sup>)

Beam	Sample 4	Sample 7	Sample 11	Sample 20	Sample 21	Sample 22
1	0.2000	0.1714	0.1470	0.1260	0.1080	0.0926
2	0.0325	0.0379	0.0442	0.0516	0.0601	0.0702
3	0.0246	0.0211	0.0181	0.0155	0.0133	0.0114
4	0.0040	0.0047	0.0054	0.0063	0.0074	0.0086

**Table 1. Fluence levels of all beams and all samples**

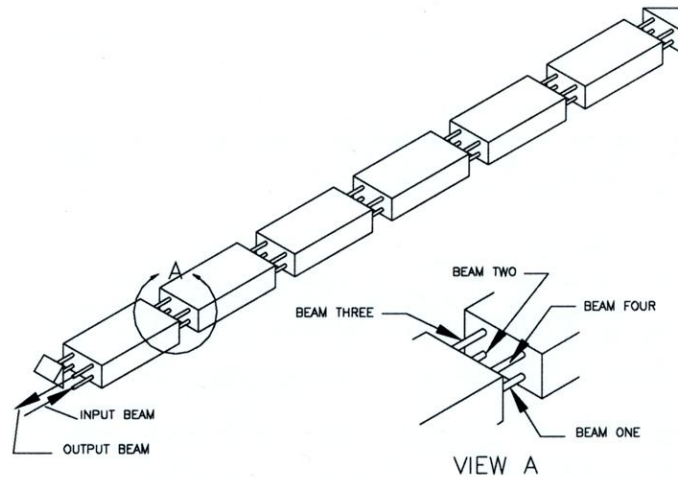


Figure 1. Test configuration

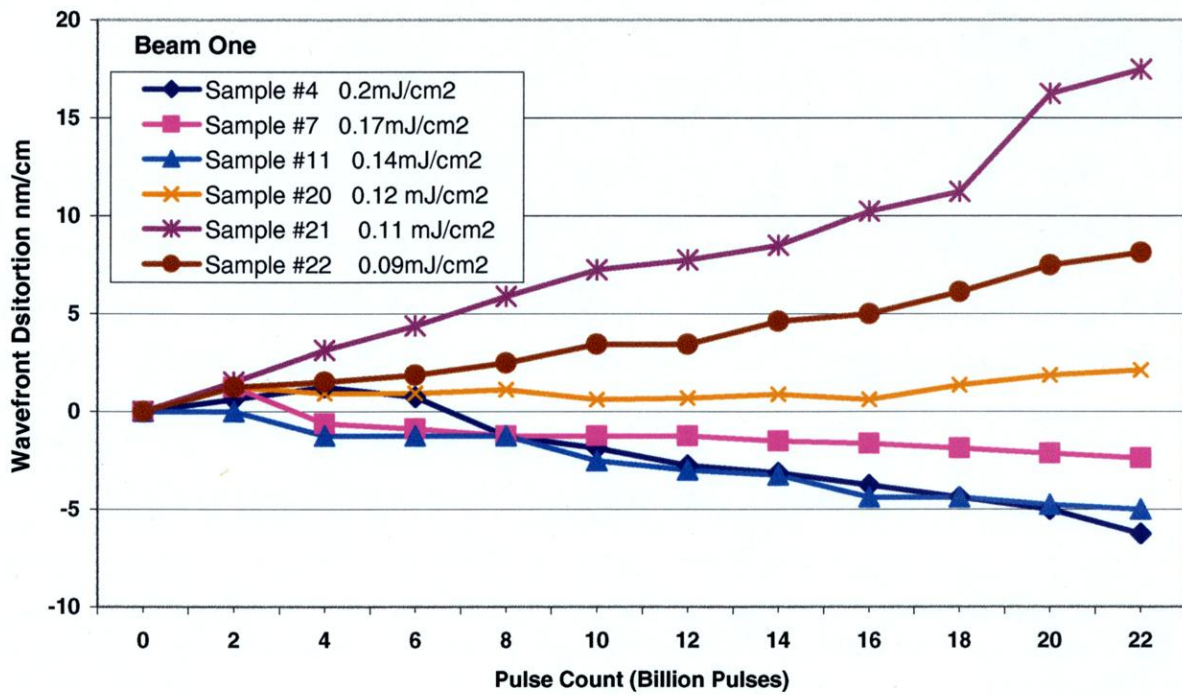


Figure 2. Wavefront distortion for samples irradiate with beam one

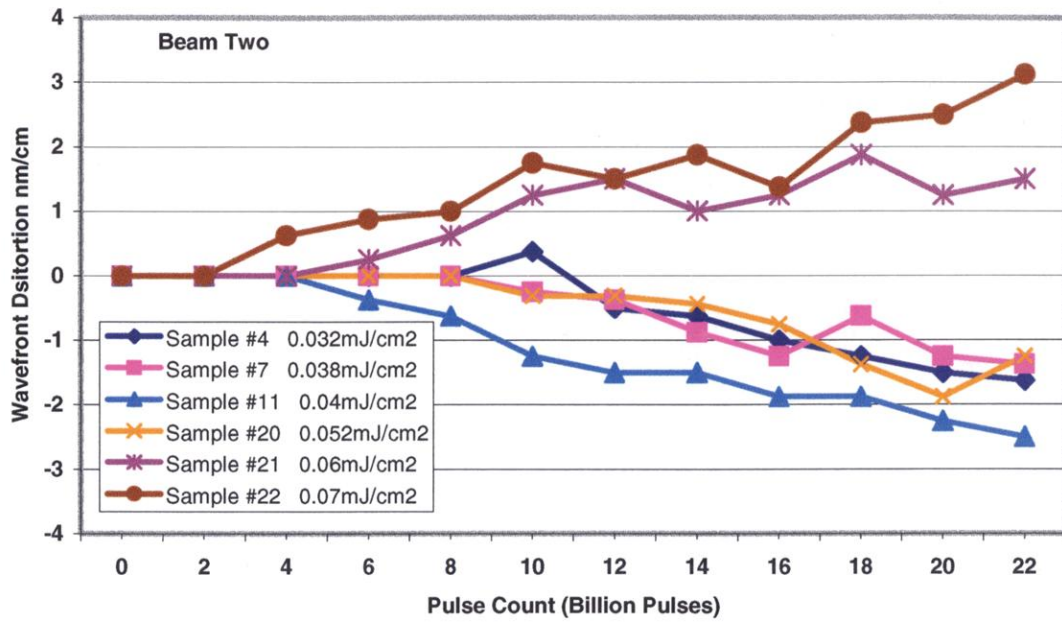


Figure 3. Wavefront distortion or samples irradiated with beam two

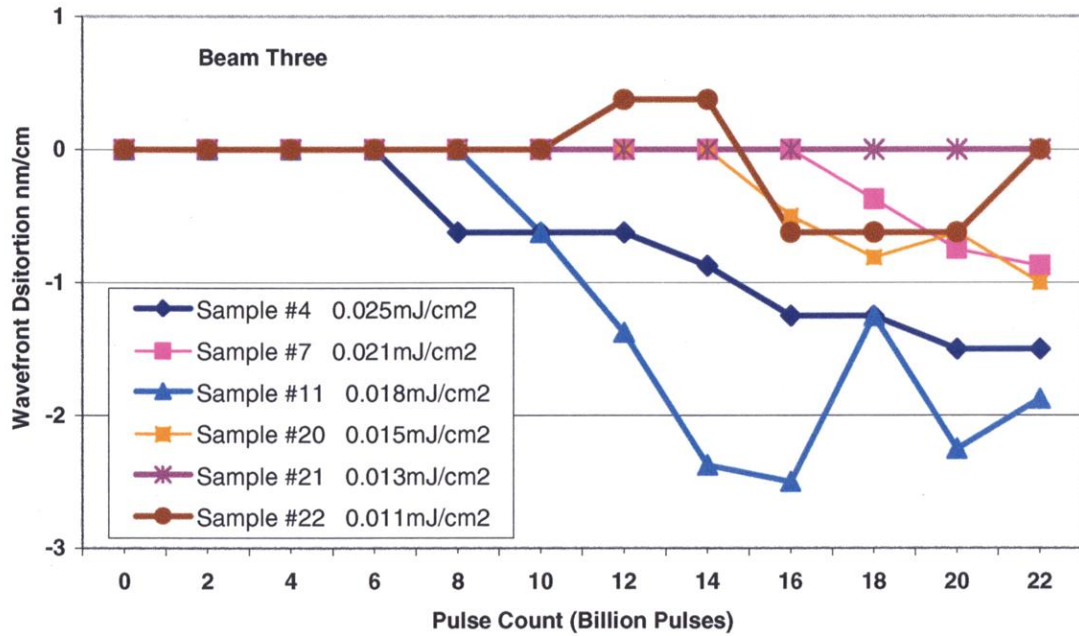


Figure 4. Wavefront distortion for samples irradiated with beam three

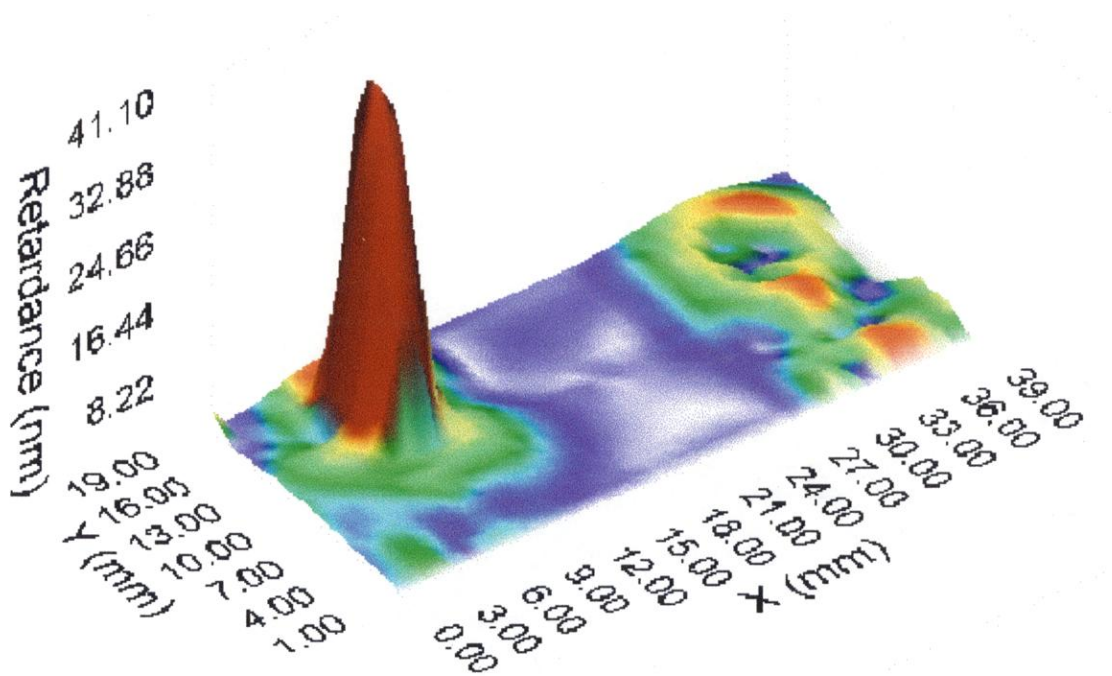


Figure 5. Birefringence of sample 4

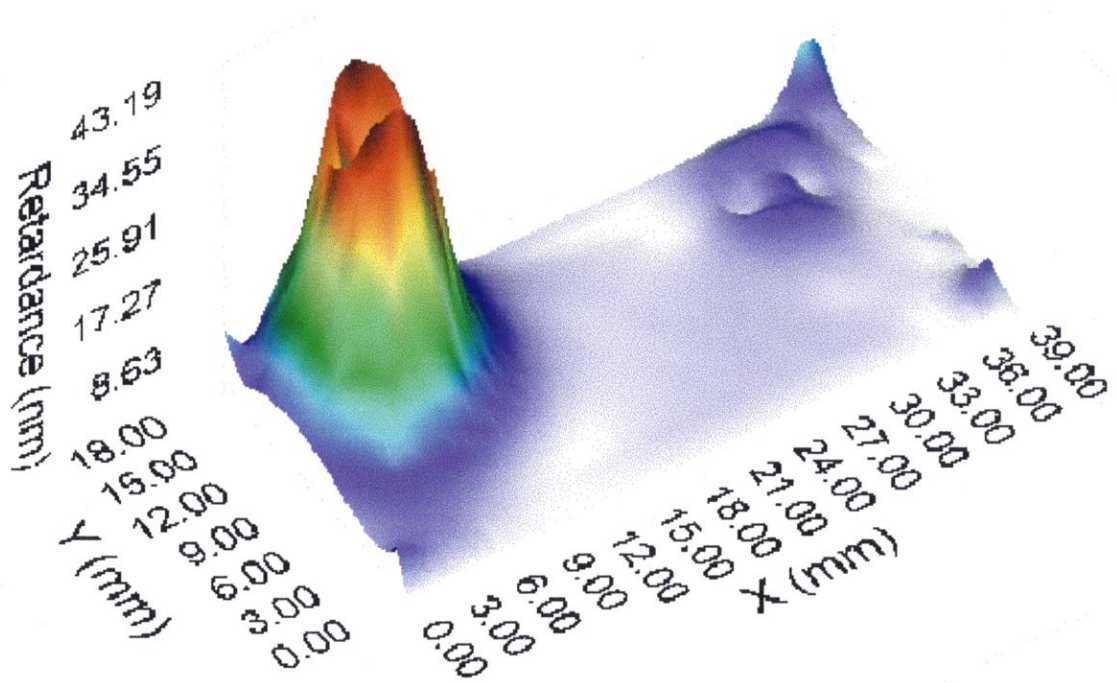


Figure 6. Birefringence of sample 21

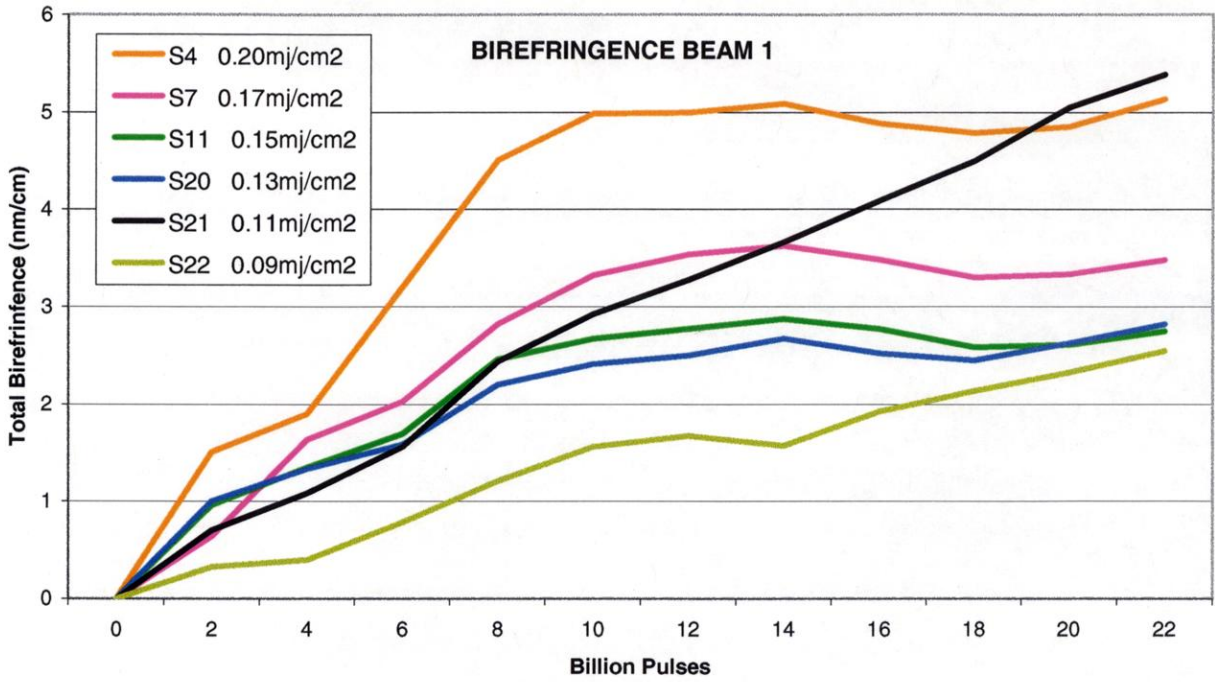


Figure 7. Birefringence of all samples

## FTIR Spectrum Analysis

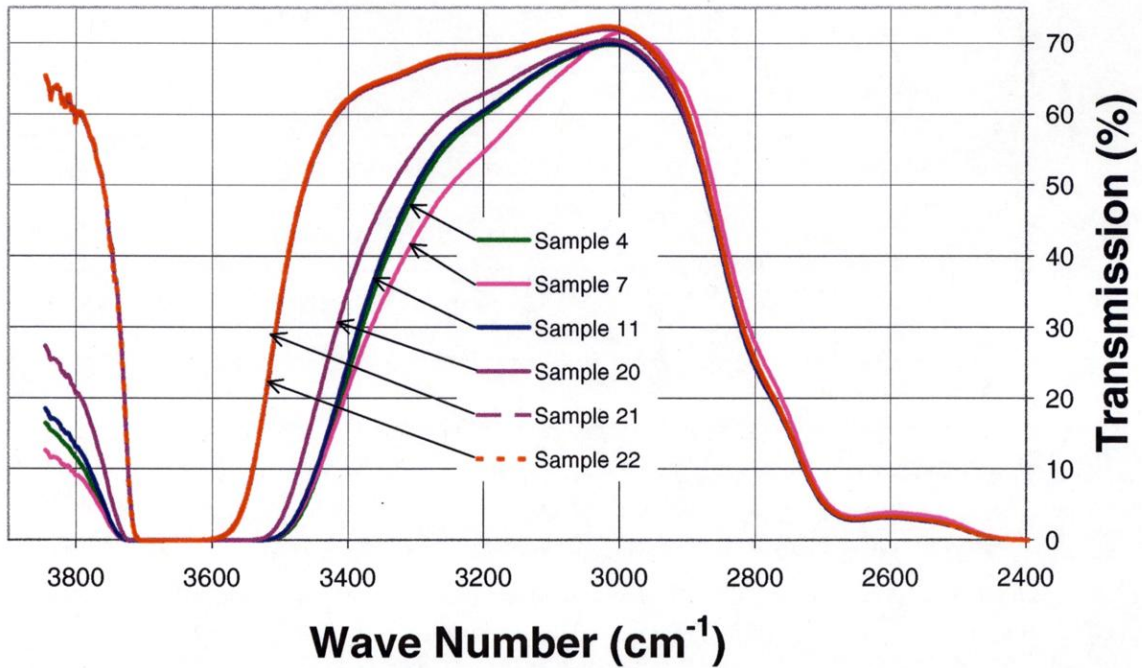


Figure 8. FTIR Spectral response

Optical-Path-Length-Change/Dose vs FTIR Spectral-Bandwidth @ 3650

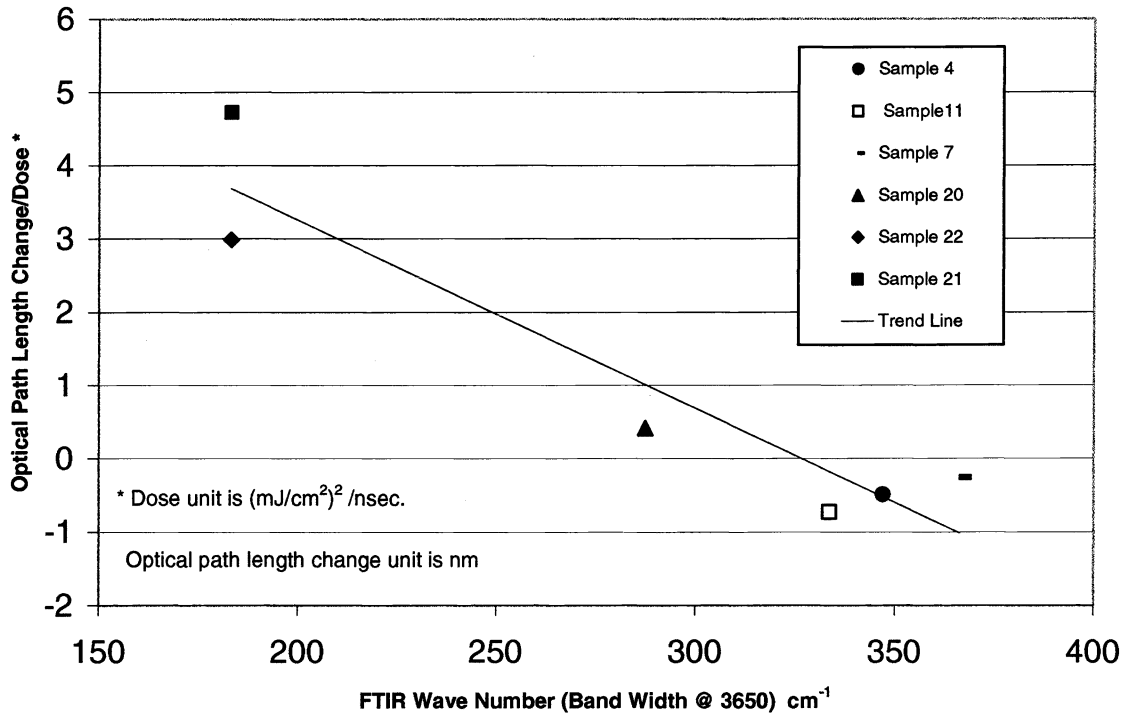


Figure 9. Optical path-length change/dose vs FTIR spectral bandwidth at  $3650\text{cm}^{-1}$